# Model of bidirectional reflectance distribution function for metallic materials

Kai Wang(王凯)[1], Jing-Ping Zhu(朱京平)[1,†], Hong Liu(刘宏)[1,2], and Xun Hou(侯洵)[1]

[1] *Key Laboratory for Physical Electronics and Devices of Ministry of Education and Shaanxi Key Laboratory of Information Photonic Technique, Xi'an Jiaotong University, Xi'an* 710049, *China*

[2] *The State Key Laboratory of Astronautic Dynamics, Xi'an Satellite Control Center, Xi'an* 710043, *China*

(Received 24 December 2015; revised manuscript received 29 April 2016; published online 20 July 2016)

Based on the three-component assumption that the reflection is divided into specular reflection, directional diffuse reflection, and ideal diffuse reflection, a bidirectional reflectance distribution function (BRDF) model of metallic materials is presented. Compared with the two-component assumption that the reflection is composed of specular reflection and diffuse reflection, the three-component assumption divides the diffuse reflection into directional diffuse and ideal diffuse reflection. This model effectively resolves the problem that constant diffuse reflection leads to considerable error for metallic materials. Simulation and measurement results validate that this three-component BRDF model can improve the modeling accuracy significantly and describe the reflection properties in the hemisphere space precisely for the metallic materials.

**Keywords:** bidirectional reflectance distribution function, metallic materials, scattering

**PACS:** 42.25.Gy, 78.20.Bh, 78.66.Bz **DOI:** 10.1088/1674-1056/25/9/094201

## 1. Introduction

For precisely describing the reflection behaviors of surfaces, the bidirectional reflectance distribution function (BRDF) has been widely used in optical remote sensing,[1] object detection and recognition,[2] environmental monitoring,[3] and other fields of scientific research.[4] The BRDF models can be divided into two classes:[5] empirical and analytical. The empirical model relies mainly on experience and experimental data,[6] while the analytical model is based on a first-principles modeling approach. Typically, most models are hybrid, instead of purely analytical or empirical. Moreover, the analytical model can be further divided into the physical optics model based on Kirchhoff approximation[7,8] and geometrical optics models based on microfacet theory.

Most surfaces are neither ideal specular reflectors nor ideal diffuse reflectors. A geometrical optics model, which assumes that the surface consists of small, randomly disposed mirror-like microfacets, was proposed by Torrance and Sparrow.[9] Specular reflection from these facets plus a diffuse component which is assumed to be perfect Lambertian due to multiple reflections was postulated as the basic mechanism of the reflection process. Phong simplified the Torrance–Sparrow (T–S) model and proposed a reflectance model that was a linear combination of specular and diffuse reflection. This model is the first description for non-Lambertian surfaces and is a well-known class of BRDF models based on cosine lobes.[10] A reflectance model proposed by Cook incorporated the Fresnel term into the T–S model to capture the wavelength dependency of the first surface reflection.[11] He presented a sophisticated analytical BRDF model[12] based on physical optics for isotropic materials.[13,14] This model considers important phenomena associated with the wave-like nature of light such as diffraction and interference. However, the model is cumbersome to compute and the values of the parameters required by the model are not always easily obtainable. Based on the T–S model and probability and statistics, Wu presented a five-parameters statistical model.[15] It simplifies the experimental measurement and can avoid the problem of acquiring the roughness parameter and optical constant of samples for rough surfaces and coatings. This model is optimized by genetic algorithms to study the 1D conducting and dielectric rough surface in the microwave band.[16,17] A new semi-empirical seven-parameter BRDF model based on a five-parameter statistical model was developed in the UV band with measured data.[18] Wang presents a six-parameter model through fitting processing of measured data based on the simulated annealing algorithm.[19]

All of above models divide the reflected light into a specular component and a diffuse reflection component which follows the Lambert law. Unfortunately, most of our tests for metallic materials show that there are considerable errors if the diffuse reflection is a constant. Aiming to address these defects, a BRDF model based on a three-component assumption is presented.

## 2. Three-component BRDF model

The bidirectional reflectance distribution function (BRDF) denotes the basic optical properties and describes

†Corresponding author. E-mail: jpzhu@mail.xjtu.edu.cn

© 2016 Chinese Physical Society and IOP Publishing Ltd 

the distribution of the reflected energy in the hemisphere. It is defined as[20]

$$f(\theta_i, \phi_i; \theta_r, \phi_r) = \frac{dL_r(\theta_r, \phi_r)}{dE_i(\theta_i, \phi_i)} \ (sr^{-1}), \tag{1}$$

where $(\theta_i, \phi_i)$ and $(\theta_r, \phi_r)$ denote the directions of incident and reflected beams, respectively, the angel $\alpha$ is the polar angle from the mean surface normal to the microfacet normal $\boldsymbol{n}$, $\beta$ is the incident angle onto and reflected angle from a microfacet as measured from the microfacet normal. Radiance $dL_r$ is the radiant power flow per unit solid angle and unit area normal to the rays, and irradiance $dE_i$ is the power flux density irradiating a surface per unit area of the surface. The geometry of the incident and reflected beams is shown in Fig. 1.

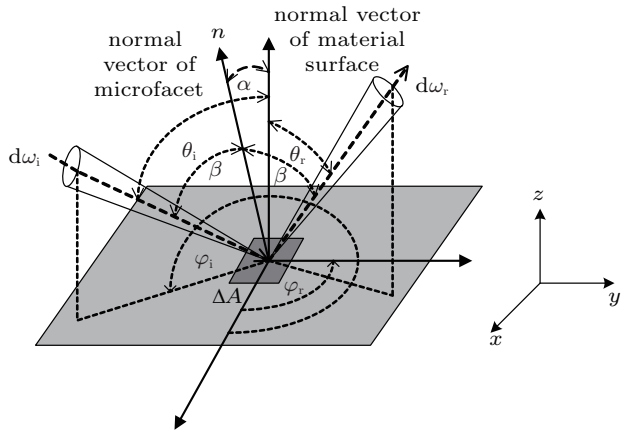



**Fig. 1.** Geometric illustration of angle variables for description of a BRDF.

Most geometrical optics BRDF models considered scattered radiance as the sum of specular radiance and diffuse radiance. Although diffuse reflection was considered as a sum of multiple reflection and volume scattering by many researchers, both of the two parts were treated as Lambertian reflection. Unfortunately, these models with two-component assumption do not agree well with experimental results of metallic materials. Therefore, we analyze the physical mechanism of the interaction between the light and object, and divide the reflect light into three components: specular reflection, directional diffuse reflection, and ideal diffuse reflection. The three-component assumption describes the reflection process with more detail and accuracy, as shown in Fig. 2.

The specular reflection, directional diffuse reflection, and ideal diffuse reflection are denoted by $f_s$, $f_{dd}$, and $f_{id}$, respectively. Therefore, the BRDF expression reads

$$f = k_s f_s + k_{dd} f_{dd} + k_{id} f_{id}, \tag{2}$$

where $k_s$, $k_{dd}$, and $k_{id}$ are the coefficients of the three components, respectively.

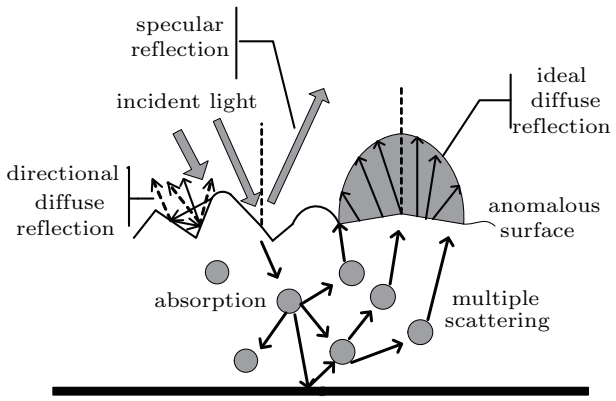



**Fig. 2.** Interaction between the light and object.

Specular reflection is considered according to the microfacet theory in which each microfacet agrees with Snell's law and its slope follows Gaussian distribution. The BRDF expression of the specular reflection $f_s$ can be given by[9]

$$f_s = \frac{1}{2\pi}\frac{1}{4\sigma^2}\frac{1}{\cos^4(\alpha)}\frac{\exp(-\tan^2(\alpha)/2\sigma^2)}{\cos(\theta_r)\cos(\theta_i)}G(\theta_i, \theta_r, \varphi), \tag{3}$$

where $G$ is the geometrical attenuation factor[21] that accounts for shadowing/masking.

$$G(\theta_i, \theta_r, \varphi) = \min\left(1, \frac{2\cos\alpha\cos\theta_r}{\cos\beta}, \frac{2\cos\alpha\cos\theta_i}{\cos\beta}\right). \tag{4}$$

The directional diffuse reflection (also called multiple reflection) is formed by the light rebounding many times on the uneven surface of the sample. This part was assumed to be uniformly distributed in hemisphere space in the existing model. However, it does not fit well with our measurements in which the directional diffuse reflection of metallic materials reaches the peak value around 0° reflection angle and has smaller values with a larger reflection angle. The spatial distribution of the multiple reflected light is not homogeneous for metallic materials, and we find that $f_{dd}$ follows a Gaussian distribution from our measurement results. The expression of $f_{dd}$ is given by

$$f_{dd} = \frac{1}{\sqrt{2\pi}\sigma_m}\exp(-\theta_r^2/2\sigma_m^2), \tag{5}$$

where the parameter $\sigma_m$ is acquired by fitting it with the experimental data.

Ideal diffuse reflection is formed by the beam that enters into sample subsurface, interacts with the interior material, and penetrates the surface. $f_{id}$ is homogeneous in the entire hemisphere, so it is a constant, i.e.,

$$f_{id} = 1. \tag{6}$$

## 3. Test and validation

### 3.1. Determination of parameters

Three typical kinds of metal materials, Al, Cu, and Fe, are measured using a Dimension ICON piezoresponse force microscope which is produced by BRUCKER Corporation.

The surface roughness of Cu and Fe are $\sigma_{Cu} = 0.070$ μm and $\sigma_{Fe} = 0.115$ μm, respectively. In addition, three Al samples with a different surface roughness ($\sigma_{Al} = 0.087$ μm, 0.142 μm and 0.782 μm) are chosen to validate the three-component BRDF model. The device and metallic samples are shown in Fig. 3.

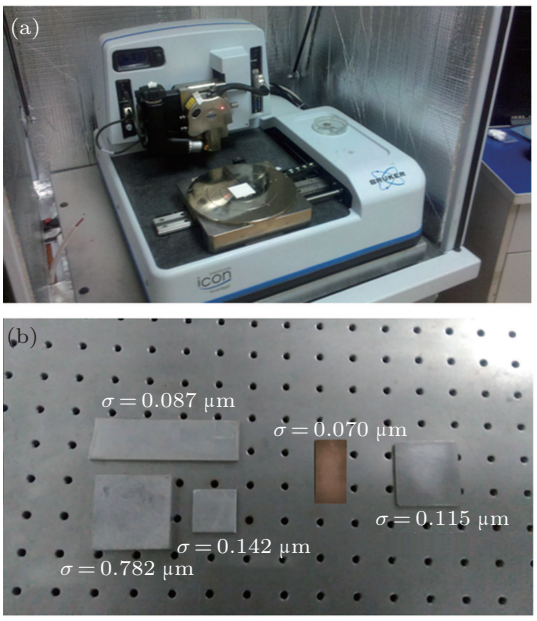



**Fig. 3.** (color online) (a) Piezoresponse force microscope and (b) metallic materials: Al (left) with different roughness, Cu (middle) and Fe (right).

The experimental setup consists of a 632.8 nm laser, an LM-5 silicon probe laser power meter, a turntable measurement and control unit. It is schematically shown in Fig. 4.

In the experiment, the distance of illumination and detection for the measured sample kept a constant value in different angles. Thus, the paths of both the laser and detector are two semicircles with one center of the circle. The laser source was fixed to $\theta_i = 0°$ (the direction illuminates the sample surface vertically). The reflected light from the sample surface was received by the moving detector when the reflection angle ranged from $-80°$ to $80°$. The location of the laser source was changed every $10°$ and the operation of the detector repeats the above steps until the distribution of the reflected light in the whole plane of incidence in different incident angles ranging from $0°$ to $80°$ was acquired.

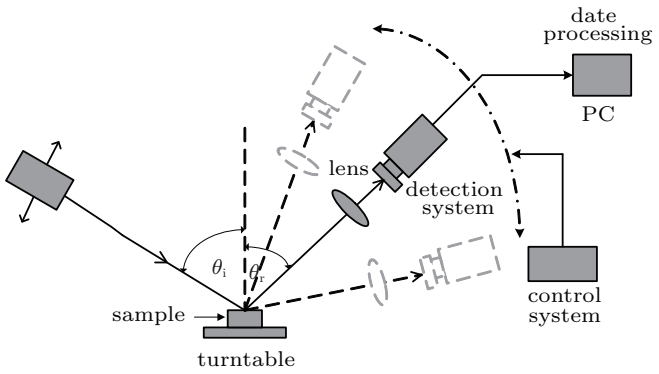



**Fig. 4.** Schematic view of the BRDF measurements.

The whole BRDF data in different reflection angles from $-80°$ to $80°$ with a step of $10°$ in the plane of incidence can be acquired when the illumination zenith angle ranges from $0°$ to $80°$ with the same step as the reflection angles. The parameters $k_s$, $k_{dd}$, and $k_{id}$ of the three metallic samples in different angular conditions were analyzed and determined by matching measured data. It was found that $k_{dd}$, $k_{id}$, and $\sigma_m$ are invariable in different incident angles for the three metallic samples, while the amplitude of the peak value of $f_s$ strengthened distinctly with the increase of $\theta_i$. We find that $k_{dd} = 900$, $k_{id} = 25$, and $\sigma_m = 0.7$ are best fitting parameters for the three samples. The $k_s$ of Al with different surface roughness $\sigma$, Cu and Fe in different incident angles are shown in Tables 1 and 2.

From Tables 1 and 2, we find that $k_s$ is different for different metallic materials as well as for the same metallic material with different surface roughness.

Thus, the complete expression of BRDF model can be written as

$$f = k_s \frac{1}{2\pi}\frac{1}{4\sigma^2}\frac{1}{\cos^4(\alpha)}\frac{\exp(-\tan^2(\alpha)/2\sigma^2)}{\cos(\theta_r)\cos(\theta_i)}G(\theta_i,\theta_r) + 900\frac{1}{\sqrt{2\pi}\sigma_m}\exp(-\theta_r^2/2\sigma_m^2) + 25. \quad (7)$$

**Table 1.** The parameter $k_s$ of Al with different surface roughness.

| Incident angle $\theta_i$ | 0° | 10° | 20° | 30° | 40° | 50° | 60° | 70° | 80° |
|---|---|---|---|---|---|---|---|---|---|
| $\sigma = 0.087$ μm | 508 | 532 | 565 | 590 | 615 | 636 | 660 | 685 | 711 |
| $\sigma = 0.142$ μm | 280 | 300 | 350 | 380 | 400 | 400 | 400 | 425 | 475 |
| $\sigma = 0.782$ μm | 50 | 66 | 80 | 102 | 125 | 142 | 160 | 178 | 198 |

**Table 2.** The parameter $k_s$ of different metallic materials.

| Incident angle $\theta_i$ | 0° | 10° | 20° | 30° | 40° | 50° | 60° | 70° | 80° |
|---|---|---|---|---|---|---|---|---|---|
| Al $\sigma = 0.142$ μm | 280 | 300 | 350 | 380 | 400 | 400 | 400 | 425 | 475 |
| Cu $\sigma = 0.070$ μm | 100 | 135 | 165 | 190 | 215 | 245 | 260 | 300 | 320 |
| Fe $\sigma = 0.115$ μm | 115 | 130 | 145 | 165 | 185 | 200 | 215 | 237 | 260 |

The normalized BRDF of the three-component model and measurements for metallic Fe in different incident angles is shown in Figs. 5(a)–5(c). It shows that this model fits well with the measurements.

### 3.2. Validation of three-component BRDF model

In order to validate the three-component BRDF model given in this paper, the BRDF of Al with different surface roughness $\sigma$ and Cu were measured for $\theta_i = 20°$, 40°, and 60°. The simulation and measurement results are compared as shown in Fig. 6. Note that $f/f(\theta_i)$ in the figure are normalized with respect to their values at the specular angles ($\theta_i = \theta_r$). Observation of both of the two model predictions is in the specular plane ($|\varphi_i - \varphi_r| = \pi$).

Figures 6(a), 6(c), and 6(e) show the value of $f/f(\theta_i)$ for Al with different surface roughness. We find that the diffuse reflection accounts for a higher proportion at different incident angles when the surface roughness is larger, i.e., $\sigma = 0.782$ μm. The diffuse reflection we present matches well with the measurements. When the surface roughness is small, the results show that the specular reflection peak increases gradually with the incident angle for both metallic materials. The BRDF curve is sharper for larger incident angles, which indicates that the reflected energy is more concentrated. Furthermore, the directional diffuse reflection is stronger when $\theta_r$ is around 0° and it drops off at larger reflect angles. This also indicates that the larger the surface roughness is, the smaller and smoother the specular peak is at the same incident angle. Finally, the three-component model and T–S model of the two metallic samples for $\theta_i = 20°$, 40°, and 60° are compared. Compared with measurements, the root mean square error (RMSE) of T–S model (RMSE1) and RMSE of three-component model (RMSE2) for $\theta_i = 20°$, 40°, and 60° are given in Table 3.

It shows that our three-component model significantly improves the modeling accuracy of BRDF and can accurately describe the distribution characteristics of the reflected energy of the metallic material in the hemisphere, although the error between the model and measured data still exists at large reflected angles. We will decrease the error of the BRDF model when incidence is approaching the grazing angle in the future.

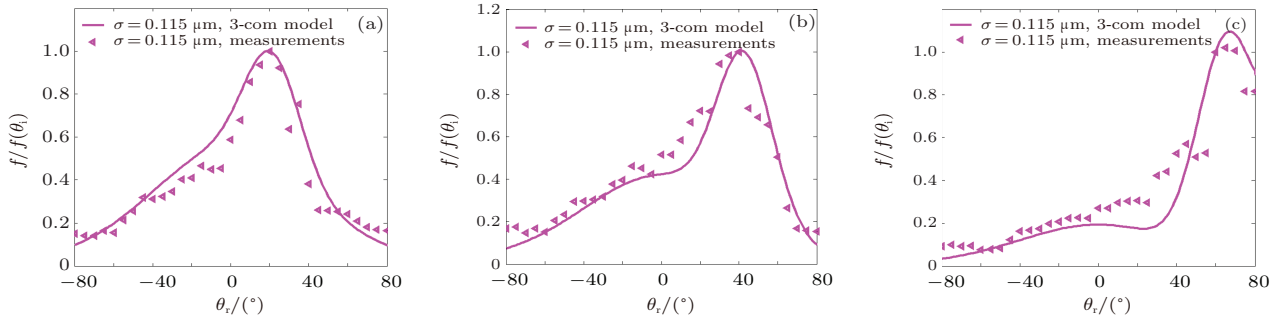



**Fig. 5.** (color online) Relationship of normalized BRDF and reflected angle at different incident angles for Fe (a) $\theta_i = 20°$, (b) $\theta_i = 40°$, (c) $\theta_i = 60°$.

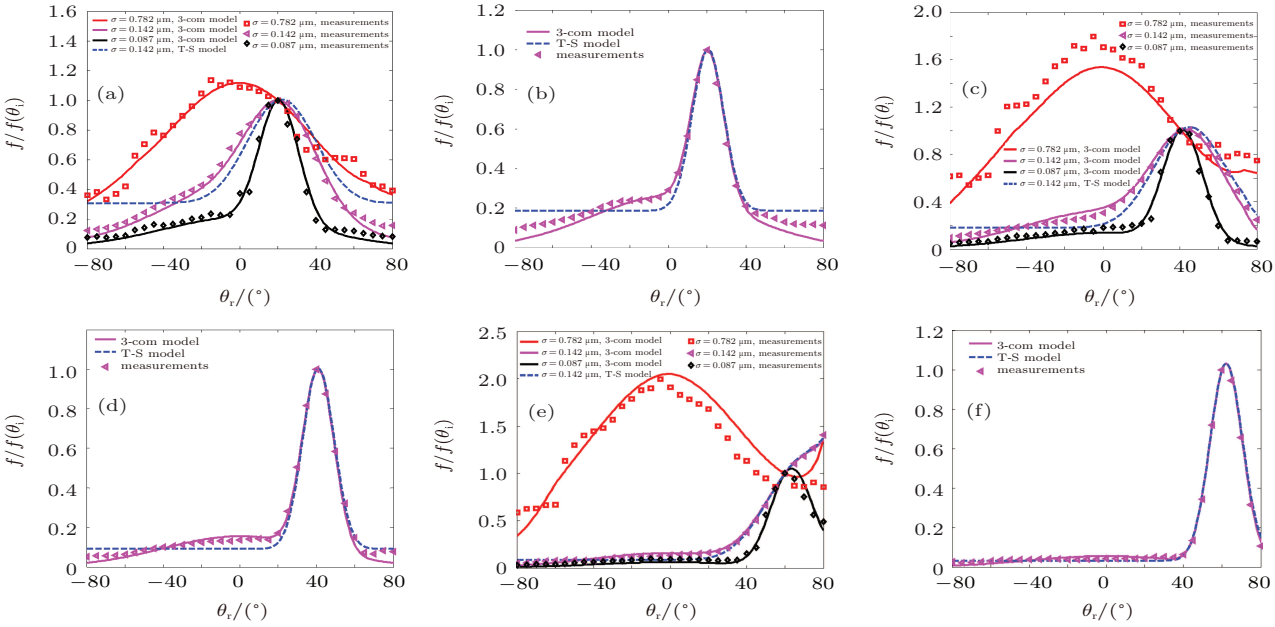



**Fig. 6.** (color online) Relationship of normalized BRDF and reflected angle at different incident angles. (a) Incident angle 20°Al with different σ; (b) incident angle 20° Cu; (c) incident angle 40° Al with different σ; (d) incident angle 40° Cu; (e) incident angle 60° Al with differentσ; and (f) incident angle 60° Cu.

**Table 3.** The RMSE between two models and measurements.

| | Al | | | Cu | | |
|---|---|---|---|---|---|---|
| | 20° | 40° | 60° | 20° | 40° | 60° |
| RMSE1 | **0.4860** | **0.0584** | **0.0310** | 0.2272 | 0.0308 | 0.0192 |
| RMSE2 | **0.1702** | **0.0395** | **0.0221** | 0.1723 | 0.0229 | 0.0155 |
| Percent decrease | **65.00%** | **32.36%** | **28.61%** | 24.17% | 25.79% | 19.15% |

## 4. Conclusion

A three-component BRDF model with specular reflection, directional diffuse reflection, and ideal diffuse reflection is presented. The specular reflection component is given by microfacet theory. Directional diffuse reflection is assumed as Gaussian distribution from measurements and ideal diffuse reflection is uniform distribution. The coefficients are determined by experimental results and the expression of the three-component BRDF model is given. Three kinds of typical metallic materials with different roughnesses are measured for $\theta_i = 20°$, 40°, and 60°. Simulations and tests validate that the modeling error of T–S model has been obviously decreased by the three-component model. It indicates that the three-component BRDF model improves the modeling accuracy of the metallic materials significantly and describes the distribution characteristics of the reflected energy in the hemisphere space precisely.

## Acknowledgment

The authors would like to thank Electronic Materials Research Laboratory in Xi'an Jiaotong University for the assistance of the surface roughness measurement for the metallic materials.

## References

[1] Georgiev G T, Gatebe C K, Butler J J and King M D 2006 *SPIE Optics+ Photonics, International Society for Optics and Photonics*, p. 629603
[2] Wang O, Gunawardane P, Scher S and Davis J 2009 *Computer Vision and Pattern Recognition, IEEE*, p. 2805
[3] Otremba Z and Piskozub J 2004 *Opt. Express* **12** 1671
[4] Bai L, Wu Z S, Cao Y H and Huang X 2014 *Opt. Express* **22** 8515
[5] Montes Soldado R and Ureña Almagro C 2012
[6] Westlund H B and Meyer G W 2002 *Proceedigs - Graphics Interface*, May 27–29, 2002, Calgary, Canada, pp. 189–200
[7] Guo R P and Tao Z S 2009 *Optics & Lasers in Engineering* **47** 1205
[8] Luo W, Zhang M, Zhou P and Yin H C 2010 *Chin. Phys. B* **19** 084102
[9] Torrance K E and Sparrow 1967 *J. Opt. Soc. Am.* **57** 1105
[10] Phong B T 1975 *Communications of the ACM* **18** 311
[11] Cook R L and Torrance K E 1982 *ACM Transactions on Graphics* **1** 7
[12] Xiao D H, Kenneth E T and Fraveois X S 1991 *Computer Graphics* **25** 175
[13] Cao Y H,Wu Z S, Zhang H L, Wei Q N and Wang S M 2008 *Acta Opt. Sin.* **28** 792 (in Chinese)
[14] Wang A Q, Guo L X and Chai C 2011 *Chin. Phys. B* **20** 050202
[15] Wu Z S and Dou Y H 2003 *Acta Opt. Sin.* **23** 1250 (in Chinese)
[16] Lu J, Wang J B and Sun G C 2009 *Chin. Phys. B* **18** 1598
[17] Guo L X, Gou X Y and Zhang L B 2014 *Chin. Phys. B* **23** 114102
[18] Bai L, Wu Z S, Zou X R and Cao Y H 2012 *Opt. Express* **20** 12085
[19] Wang H Y, Zhang W and Dong A 2013 *Measurement* **46** 3654
[20] Nicodemus F E 1970 *Appl. Opt.* **9** 1474
[21] Blinn J F 1977 *ACM SIGGRAPH Computer Graphics* **11** 192